Lab on a Chip

TECHNICAL INNOVATION

View Article Online
View Journal | View Issue

CrossMark
click for updates

Cite this: *Lab Chip*, 2014, **14**, 4178

Received 26th August 2014,
Accepted 5th September 2014

DOI: 10.1039/c4lc00992d

www.rsc.org/loc

A 3D-printed microcapillary assembly for facile double emulsion generation†

Chiara Martino, Simon Berger, Robert C. R. Wootton and Andrew J. deMello*

The design, fabrication and testing of facile microcapillary device assembly, suitable for monodisperse double emulsion production is reported. The interface is fabricated in a direct and rapid manner *via* 3D printing and shown to be robust in the controllable generation of both single and double emulsions at high generation frequencies.

Introduction

Double emulsions are complex systems of immiscible liquids arranged in a way that one or more droplets of one fluid (A, the inner phase) are formed inside a droplet of another, immiscible, fluid (B, the middle phase), which is itself encapsulated in an outer phase in which B is immiscible (A or C, the outer phase) (Fig. 1a). Double emulsions have found a diversity of applications and uses in bioanalytical science,[1] chemical synthesis,[2] the generation of liposomes[3] and polymersomes[4,5] cell mimesis,[6] cosmetics[7] and in sustained release pharmaceutical formulations.[8–10] The large-scale production of monodisperse double emulsions is commonly achieved using microfluidic methodologies that rely on the use of glass[4,11] or polydimethylsiloxane (PDMS) structures.[12–14] Although glass microfluidic devices are fabricated using standard photolithographic techniques, which incur high costs and require access to sophisticated instrumentation, they can be used with almost any type of solvent and operate at a range of temperatures and pressures. This contrasts with PDMS microdevices which, although cheap and easy to produce, are employable only for a severely limited range of working phases.[15] Although recent studies have reported glass coated PDMS devices[16] and hybrid glass capillary-PDMS devices[17] that are able to withstand a variety of organic solvents, the need for microfabrication and photolithography facilities, and the incompatible physical properties of disparate substrates still limits their use. Indeed, all-glass devices for double emulsion generation must be either purchased from (a small number of) microfluidic device manufacturing companies[4] or fabricated in a laboratory *via* laborious glass etching techniques or glass capillary assembly.[11] The second method is by far the most used and the most adaptable in the production of multiple compartments of different solutions,[18] a goal difficult to obtain with the other approaches. In the current paper we report a novel glass capillary double emulsion system that avoids the drawbacks that manual glass capillary device assembly usually carries.

Introduced for the first time in 2005 by Utada *et al.*,[11] the glass microcapillary device has been widely used for the generation of monodisperse double emulsions in fields as diverse as materials science,[19,20] biology and biomedical engineering.[21,22] This system allows the formation of a double emulsion in a single emulsification step *via* the flow-induced breakup of a tri-phasic coaxial flow. The inner and middle phases flow in coaxial glass capillaries and are brought into counter-flow contact with the outer phase. This contact causes the flow to break up, forming a double emulsion. The double emulsion thus formed flows through the collection capillary, together with the outer phase, reaching the outlet of the device (Fig. 1b–c).

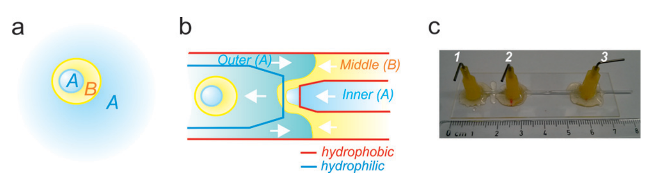

Fig. 1 Formation of double emulsions. (a) The structure of a double emulsion made of a droplet of fluid A, dispersed in an immiscible fluid B and further dispersed in fluid A. (b) Schematic of a multi-capillary device made from an outer capillary and two coaxial inner capillaries. The inner and middle phases flow coaxially and generate a double emulsion at the point where the flows meet the counter flow outer phase. Capillary surfaces require individual chemical treatment according to the type of emulsion to be formed. For instance the device shown can produce water/oil/water (W/O/W) emulsions. (c) Image of an assembled capillary device ready for use. Blunt needles are glued to the capillaries and are used as inlets for inner (1), middle (2) and outer (3) phases.

Institute for Chemical and Bioengineering, Department of Chemistry and Applied Biosciences, ETH Zurich, Vladimir-Prelog-Weg 1, Zürich 8093, Switzerland. E-mail: andrew.demello@chem.ethz.ch

† Electronic supplementary information (ESI) available: Images S1–S4; videos of emulsion generation and distance adjustment; CAD/Inventor files. See DOI: 10.1039/c4lc00992d

Despite its widespread adoption, the assembly of such microcapillary devices is laborious, operator-dependent and irreproducible. The standard fabrication method consists of inner capillary drawing and chemical surface treatment, coaxial capillary alignment, adjustment of the distance between the opposing inner capillaries and fluidic inlet interface connection. Within this fabrication process several challenges are well recognized.[23] First and foremost, the delicate alignment of the inner capillaries as well as their separation are difficult to control and even more difficult to reproduce. Second, the adhesive required for sealing inlets and outlet often blocks the glass capillaries and compromises device function. Finally the assembled device cannot readily be disassembled, cleaned and chemically retreated for reuse.

Herein, we present a novel approach for microcapillary interface fabrication that relies on lithography-free rapid prototyping and overcomes the aforementioned fabrication problems without altering the working principle of the microcapillary device. 3D printing represents an ideal fabrication technique for interface construction since it allows direct generation of complex, three-dimensional structures that are otherwise only achievable using multiple processing steps, and at significantly higher costs. Such rapid prototyping methods have proved their utility in a number of microfluidic applications.[24–27] Our approach relies on the fabrication of two connectors that hold the inner and outer capillaries in position and provide access to the contained fluids. The connectors are mounted in a specular fashion on a guide that can easily be mounted on a microscope stage. Each connector is made of two parts: a screw and a nut. The first part houses the inner capillary and is screwed onto the second part that holds the outer capillary. Significantly, the outer capillary can either be circular or square in cross-section. The screw mechanism allows a translational movement of the inner capillary on both sides that permits precise definition of the distance between the inner capillaries even while liquids are flowing (Fig. 2).

Capillary device fabrication and assembly

Glass inner capillaries (ID 0.70, OD 0.86 mm) (VitroCom, USA) were tapered using a micropipette puller (P-1000, Sutter Instruments, USA) and a microforge (MF-900, Narishige Group, Japan), whereas glass capillaries with circular (ID 1.50 mm, OD 1.80 mm) or square (ID 1.00 mm, OD 1.40 mm) cross-section were used as the outer channel. Glass surface treatment was achieved by soaking capillaries overnight in a 2% solution of *n*-octadecyltrimethoxil silane (376212, Sigma Aldrich, Germany) or 2-methoxy(polyethyleneoxy)silane (AB 111226, abcr, Germany) in isopropanol, to generate a hydrophobic or hydrophilic coating respectively. Treated capillaries were then dried with nitrogen and heated for 1 hour at 100 °C.

The capillary alignment device was designed using AutoCAD 2014 (Autodesk, USA) and printed using a Project 3510 HD (3D Systems GmbH, Germany) printer using a photo curable acrylonitrile butadiene styrene (ABS) resin. The design was made in two parts namely: the screw holding the inner capillary and the nut holding the outer capillary. The screw holder was a simple straight interface between a steel pin (Gauge 20 stainless steel blunt needle, IP720050, I and Peter Gonano, Austria) (Hole ID 0.92 mm) and the inner capillary. Both the capillary and the pin were gently pushed into the screw holder; the connection was sealed automatically due to the precise fit of the holder to the capillary and pin. The nut was fitted with a connection for the outer capillary, a second inlet for the middle/outer phase and the screw thread in which the screw holding the inner capillary was inserted. At the end of the inlet for middle/outer phase a slightly larger section was added allowing these phases to flow around the inner capillaries into the outer capillary. The section between the liquid inlet and screw thread was blocked by a narrow opening, which is just large enough to accommodate the inner capillary. The entire assembly of screw and nut was held on a rail on which the position of both holders could be freely adjusted.

After printing, the wax filling (used as a support material during 3D printing) was removed by sonicating the parts in isopropanol at 70 °C for several hours. This was followed by an additional washing step in deionized water. The cleaned parts were then assembled and connected to syringe pumps using PTFE tubing (ID 0.79 mm, OD 1.58 mm, Cole Parmer Instrument Company, USA).

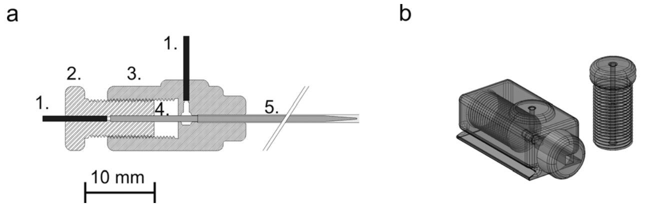

Fig. 2 Schematic of the microcapillary connector. (a) Assembly of a 2-piece connector made of: two steel pins (1), a screw (2) and a nut (3) that holds the inner and outer capillaries (4 and 5), respectively. Both pieces provide access to fluid inlets by steel pins that are connected with tubing. (b) 3D view of the screw and nut components.

Device testing and operation

The device was tested using deionized water as inner and outer fluids and Mineral oil (M3516, Sigma Aldrich, Switzerland) with 2 wt% of SPAN 80 (S670, Sigma Aldrich, Switzerland) as the middle phase. Fluids were loaded into glass syringes (1000 Hamilton gastight syringes, Switzerland) interfaced with the capillary device and mounted on syringe pumps (Aladdin Al-1000, World Precision Instruments, USA). An area scan color camera (CR-GC00-H640x, Teledyne Dalsa, Switzerland), mounted on a microscope (Axiovert 100, Zeiss, Germany), and a 2.5× objective (Epiplan-NEOFLUAR, 442310, Zeiss, Germany) were used to image and monitor droplet formation.

Sealing of the assembly was assessed by observation of any leakage when liquids were pumped into the device. Holes with circular profiles, in both the nuts and screws, showed complete integrity when operated at flow rates ranging from 1 to 110 μl min^{-1}. Occasionally, liquid leakage was observed in nuts with square profiles due to the fact that the square capillaries did not have sharp edges. In such circumstances, the polymer/glass interface could be sealed using a few drops of acrylic glue (Acrifix 116, Evonik Industries, Germany), which could be easily removed when the device was disassembled and soaked in acetone. Fig. 3 shows the final 3D printed assembly whereas Fig. S1 (ESI†) shows inner capillaries in both a square and a round outer capillary. Performance of the screw movement was assessed by observing and measuring the travel distance of the inner capillary in response to fine screw rotation. Using this method, the smallest distance that the capillary could travel within the assembly after fine manual rotation of the screw was calculated to be 2.4 μm. A video of the manually operated intercapillary distance adjustment is provided in the ESI† and clearly demonstrates the maintenance of coaxial alignment.

In addition, to assess the reproducibility of capillary alignment within the assembly, the offsets of capillary centers both in our assembly and in the commonly used epoxy-based assembly were measured. This analysis indicated that that epoxy fittings can have an offset of up to 42% in normal construction whereas the 3D-printed assembly showed a maximal offset error of 10%. Details of the measurements are provided in the Fig. S2 (ESI†).

Device operation was characterized using a square glass capillary (OD 1.4 mm–ID 1.0 mm) and two round glass capillaries (OD 0.87 mm–ID 0.70 mm) with tapered tip diameters of 24 and 185 μm. The coaxial relationship of the inner capillaries was verified from microscopic images and the distance between capillaries adjusted manually by rotation of the screws and set to three discrete distances as shown in Fig. 4a.

For these three configurations, the middle and outer phase flow rates were kept constant at 10 and 110 μl min^{-1} respectively, whereas the inner phase flow rate was varied between 1 and 10 μl min^{-1}. It was observed that stable double emulsion generation occurred only for a few combinations of input flow rates. Configuration I produced stable double emulsions with only 1 inner droplet when the inner flow rate was set at 3 μl min^{-1} (Fig. 4b); configuration II generated double emulsions with both 1 and 2 encapsulated droplets when the inner flow rate was set respectively at 3 and 9 μl min^{-1} (Fig. 4c–d) and configuration III generated only stable double emulsions containing 3 droplets for an inner flow equal to 8 μl min^{-1} (Fig. 4e). Videos of stable droplet generation were analysed to assess the inner droplet

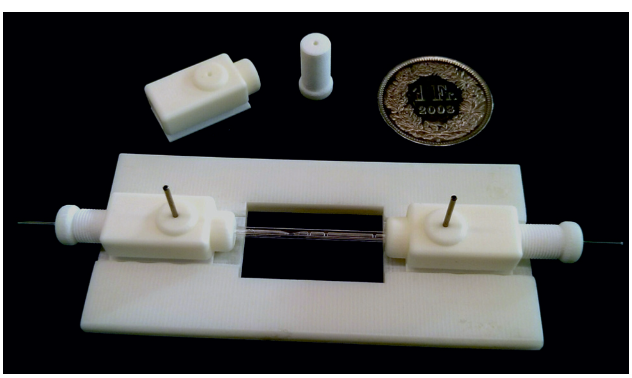

Fig. 3 A 3D-printed assembled capillary device ready for use. The connectors were mounted on a 7.40 × 3.40 mm support designed to fit on a standard microscope stage.

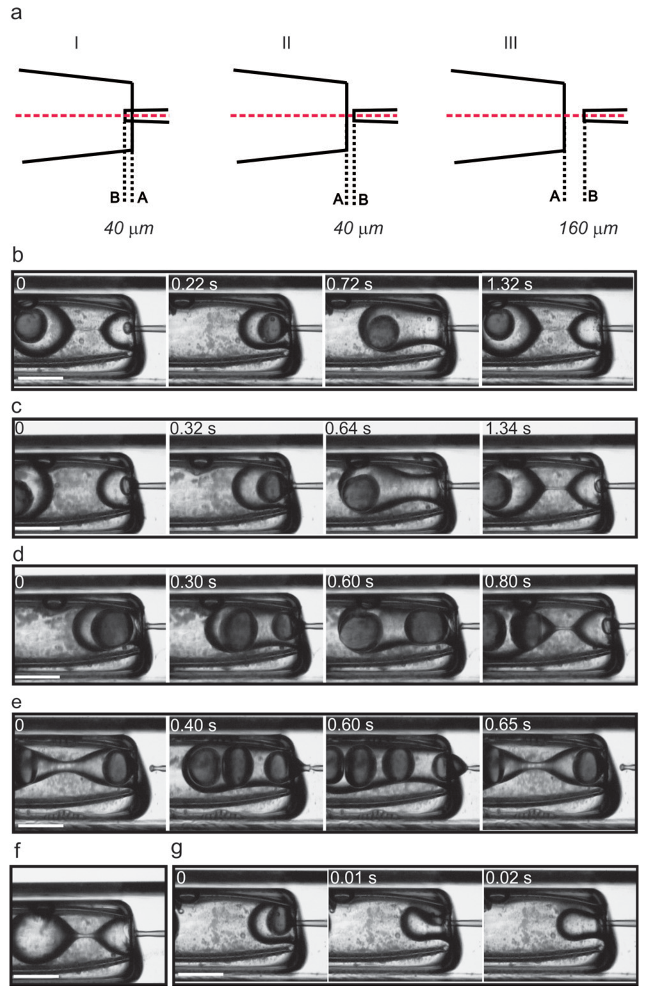

Fig. 4 Assessment of device operation through variation of the intercapillary distance. (a) The distance between the capillaries was varied and produced three configurations, which were tested for double emulsion generation. For each configuration, middle and outer phase flow rates were maintained at 10 and 110 μl min^{-1} respectively, whereas the inner fluid flow rate was varied from 1 to 10 μl min^{-1}. Stable double emulsions were produced at particular flow rate sets. (b) Configuration I: stable double emulsion generation, with single droplet encapsulation, occurring when the inner flow rate was set at 3 μl min^{-1}; (c–d) configuration II: stable double emulsion generation, with single and double encapsulation, occurring when the inner flow rate was set respectively at 3 and 9 μl min^{-1}. (e) Configuration III: stable double emulsion generation, with triple droplet encapsulation, occurring when the inner flow rate was set at 8 μl min^{-1}. (f–g) Oil droplet generation and water phases merging episodes. Scale bar equal to 500 μm.

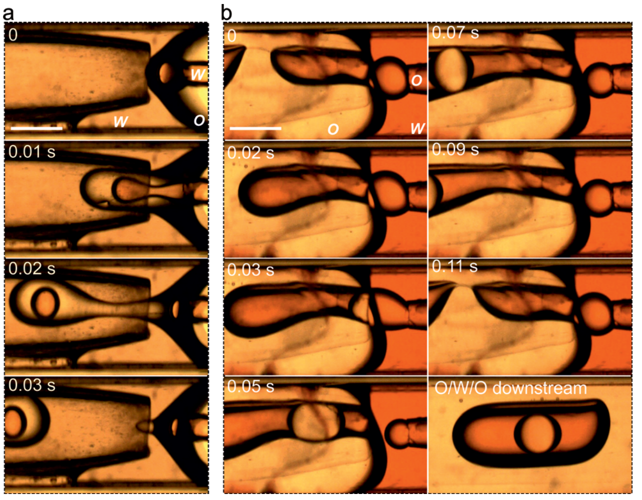

Fig. 5 Device reusability. (a) W/O/W emulsion generation achieved by localised treatment of the inner, outer and collection capillary. The intercapillary distance was set at approximately 330 μm whereas the inner, middle and outer phase flow rates were set respectively at 8, 30 and 200 μl min^{-1}. (b) O/W/O emulsion generation after device disassembly and chemical treatment of the capillaries. The device was reassembled and the intercapillary distance was set at approximately 370 μm. Flow rates of inner, middle and outer phase were set at 50, 50 and 7 μl min^{-1}. Scale bar equal to 500 μm.

dispersity (provided in the ESI†). Moreover it was observed that single encapsulation achieved in configuration I was 20 ms faster than that obtained with configuration II but produced inner droplets with a larger coefficient of variation (Table S1†). For other flow rates values herein mentioned, a combination of double emulsion together with oil droplet generation and/or water phase merging occurred (Fig. 4f and g).

The complete flow rate dependence of these formation domains, for each configuration, is graphically summarized in Fig. S3.†

Finally, the reusability of our device was assessed by producing W/O/W emulsions, then disassembling the device, chemically retreating the component capillaries, reassembling the device and then producing a O/W/O emulsion. Fig. 5 shows the double emulsions obtained before and after the disassembly and chemical re-treatment.

Conclusions

We have described a novel and simple approach for the assembly of a microcapillary device used for double emulsion generation. The interface provides for facile coaxial alignment of inner capillaries and variation of their reciprocal distance through rotation of the screws to which the capillaries are secured. Importantly, the advantages introduced by the proposed approach extend to device reusability, reduced waste and setup time. Moreover, the assembly strategy presented herein can be achieved through the use of milling techniques and the adoption of more resistant materials such as PEEK (shown in Fig. S4 in ESI†), aluminium or steel. Furthermore, the screw mechanism is well suited to interconnection with motors able to finely tune the distance between the inner capillaries, a desirable feature for industrial assembly. Finally, the use of just one connector housing the inner and the outer capillary can be employed for the formation of single emulsions, or as a droplet dispenser, which can also be converted into a micropipette system when the flow of the inner capillary is reversed. The droplet dispenser represents a cost-effective solution for single emulsion generation when photolithographic methods are inaccessible or solvents not compatible with PDMS are in use.

Acknowledgements

This project was partially supported by the ETH Zurich Postdoctoral Fellowship Program and Marie Curie Actions for People COFUND Program and by the Swiss National Science Foundation Grant CR2312-146328. Authors are also grateful to Professor Andre Studart and Mr Philipp Wei Chen for the use of micropipette puller and microforge.

Notes and references

1 K. Bernath, M. Hai, E. Mastrobattista, A. D. Griffiths, S. Magdassi and D. S. Tawfik, *Anal. Biochem.*, 2004, **325**, 151–157.
2 J. A. Hanson, C. B. Chang, S. M. Graves, Z. Li, T. G. Mason and T. J. Deming, *Nature*, 2008, **455**, 85–88.
3 H. C. Shum, D. Lee, I. Yoon, T. Kodger and D. A. Weitz, *Langmuir*, 2008, **24**, 7651–7653.
4 C. Martino, L. Horsfall, Y. Chen, M. Chanasakulniyom, D. Paterson, A. Brunet, S. Rosser, Y.-J. Yuan and J. M. Cooper, *ChemBioChem*, 2012, **13**, 792–795.
5 E. Lorenceau, A. S. Utada, D. R. Link, G. Cristobal, M. Joanicot and D. A. Weitz, *Langmuir*, 2005, **21**, 9183–9186.
6 D. A. Hammer and N. P. Kamat, *FEBS Lett.*, 2012, **586**, 2882–2890.
7 K. Yoshida, T. Sekine, F. Matsuzaki, T. Yanaki and M. Yamaguchi, *J. Am. Oil Chem. Soc.*, 1999, **76**, 195–200.
8 A. Fechner, A. Knoth, I. Scherze and G. Muschiolik, *Food Hydrocolloids*, 2007, **21**, 943–952.
9 E. Dickinson, *Food Biophys.*, 2011, **6**, 1–11.
10 F. Meng and Z. Zhong, *J. Phys. Chem. Lett.*, 2011, **2**, 1533–1539.
11 A. S. Utada, E. Lorenceau, D. R. Link, P. D. Kaplan, H. A. Stone and D. A. Weitz, *Science*, 2005, **308**, 537–541.
12 S. Okushima, T. Nisisako, T. Torii and T. Higuchi, *Langmuir*, 2004, **20**, 9905–9908.
13 S.-H. Huang, W.-H. Tan, F.-G. Tseng and S. Takeuchi, *J. Micromech. Microeng.*, 2006, **16**, 2336.
14 V. Barbier, M. Tatoulian, H. Li, F. Arefi-Khonsari, A. Ajdari and P. Tabeling, *Langmuir*, 2006, **22**, 5230–5232.
15 J. N. Lee, C. Park and G. M. Whitesides, *Anal. Chem.*, 2003, **75**, 6544–6554.
16 J. Thiele, A. R. Abate, H. C. Shum, S. Bachtler, S. Förster and D. A. Weitz, *Small*, 2010, **6**, 1723–1727.

17 W.-C. Jeong, M. Choi, C. H. Lim and S.-M. Yang, *Lab Chip*, 2012, **12**, 5262–5271.

18 H. C. Shum, Y.-J. Zhao, S.-H. Kim and D. A. Weitz, *Angew. Chem.*, 2011, **123**, 1686–1689.

19 C.-H. Chen, R. K. Shah, A. R. Abate and D. A. Weitz, *Langmuir*, 2009, **25**, 4320–4323.

20 R. K. Shah, H. C. Shum, A. C. Rowat, D. Lee, J. J. Agresti, A. S. Utada, L.-Y. Chu, J.-W. Kim, A. Fernandez-Nieves, C. J. Martinez and D. A. Weitz, *Mater. Today*, 2008, **11**, 18–27.

21 C. Martino, S.-H. Kim, L. Horsfall, A. Abbaspourrad, S. J. Rosser, J. Cooper and D. A. Weitz, *Angew. Chem., Int. Ed.*, 2012, **51**, 6416–6420.

22 H. C. Shum, A. Bandyopadhyay, S. Bose and D. A. Weitz, *Chem. Mater.*, 2009, **21**, 5548–5555.

23 A. R. Abate and D. A. Weitz, *Small*, 2009, **5**, 2030–2032.

24 O. H. Paydar, C. N. Paredes, Y. Hwang, J. Paz, N. B. Shah and R. N. Candler, *Sens. Actuators, A*, 2014, **205**, 199–203.

25 J. L. Erkal, A. Selimovic, B. C. Gross, S. Y. Lockwood, E. L. Walton, S. McNamara, R. S. Martin and D. M. Spence, *Lab Chip*, 2014, **14**, 2023–2032.

26 A. I. Shallan, P. Smejkal, M. Corban, R. M. Guijt and M. C. Breadmore, *Anal. Chem.*, 2014, **86**, 3124–3130.

27 A. K. Au, W. Lee and A. Folch, *Lab Chip*, 2014, **14**, 1294–1301.